

# Fuzzy Adaptive Sliding Mode Control for the Precision Position of Piezo-Actuated Nano Positioning Stage

Jiwen Fang<sup>1,2#</sup>, Lufan Zhang<sup>3</sup>, Zhili Long<sup>4</sup>, and Michael Yu Wang<sup>2,5</sup>

<sup>1</sup> School of Mechanical Engineering, Jiangsu University of Science and Technology, Zhenjiang, 212003, China

<sup>2</sup> State Key Lab for Manufacturing Systems Engineering, Xi'an Jiaotong University, Xi'an, 710049, China

<sup>3</sup> School of Mechanic & Electrical Engineering, Henan University of Technology, Zhengzhou, 450001, China

<sup>4</sup> Harbin Institute of Technology Shenzhen Graduate School, Shenzhen, 518055, China

<sup>5</sup> Hong Kong University of Science and Technology, Hong Kong, China

# Corresponding Author / E-mail: fjt\_617@163.com, TEL: +86-511-84445385

ORCID: 0000-0003-2277-6777

KEYWORDS: Piezo-actuated nano positioning stage, Fuzzy adaptive sliding mode control, PID sliding surface, Hysteresis compensation

*This paper concerns hysteresis and creep of a piezo-actuated nano positioning stage. The hysteresis and creep, considered as bounded disturbance or uncertainty, are suppressed without a nonlinear model. An improved Fuzzy Adaptive Sliding Mode Control (FASMC) with a Proportional-Integral-Derivative sliding surface is designed to cancel both hysteresis and creep. However, the constant slopes of the sliding function may increase oscillations. Some variable gains with adaptive rules are introduced to overcome this drawback by changing the sliding function values online. Fuzzy control is applied to tune the switching control part to improve performance. Furthermore, an adaptation law is used to approximate the optimal value of the switching control. The stability of the sliding mode control law is proved in the sense of Lyapunov stability theorem. To eliminate chattering and obtain a smooth signal, the switching control is modified and a smooth function is introduced to substitute the signum function. An anti-saturation control is introduced to keep the input voltage within safety scope. Experimental results show that FASMC can achieve faster response for step input and sinusoid signal. Both hysteresis and creep of the piezoelectric actuator are suppressed by the proposed FASMC. Therefore, the FASMC can reduce the tracking errors of the piezo-actuated stage.*

Manuscript received: March 19, 2018 / Revised: July 4, 2018 / Accepted: July 18, 2018

## 1. Introduction

The piezo-actuated nano positioning stage has become increasingly prevalent in nanopositioning applications due to the excellent advantages of high stiffness, large output mechanical force, fast response time, and extremely high resolution in displacement.<sup>1,2</sup> Nanopositioning stages with piezoelectric actuator and flexure hinges have been recognized as most appropriate platforms that utilize a piezoelectric actuator for actuation purposes.<sup>3-6</sup> These mechanisms possess several advantages over conventional mechanical systems.

However, the major problem of the piezo-actuated nano positioning stage originates from the nonlinearities in the piezoelectric actuator attributed to hysteresis and creep. Hysteresis is a nonlinear behavior between the applied electric field and the output displacement of the piezoelectric, which leads to a loss of precision positioning. Therefore, the hysteresis phenomenon must be suppressed to get high precision positioning and good tracking performance. The compensation control

for the hysteresis system has been previously reported for a wide range of application in piezoelectric actuators. Hysteresis compensation can be realized by using feedforward control with either an inverse hysteresis model or advanced control strategy without hysteresis model.

Li, Linlin proposed a new damping control with a high-gain proportional-integral controller for the piezo-actuated nano positioning stage to implement high-bandwidth operation.<sup>7</sup> A novel feedforward-nonlinear Proportional-Integral-Derivative (PID) control strategy and the inverted Preisach hysteresis compensator is proposed to eliminate hysteresis.<sup>8-10</sup> Until now, many hysteresis models have been developed,<sup>1,11</sup> such as the Preisach model,<sup>12</sup> the Prandtl-Ishlinskii model,<sup>13</sup> the Maxwell model<sup>14</sup> and the Bouc-Wen model.<sup>15</sup> Through a literature review, control techniques based on the hysteresis model have been developed to satisfy high precision requirements. Feedforward control is the common approach for the reduction of the hysteresis phenomenon. Feedforward schemes based on Coleman-Hodgdon are designed to compensate for the hysteresis of low frequency for the piezoelectric actuator.<sup>16</sup> A

hysteresis model is used to describe the piezoelectric scanner of an atomic force microscope and then an inverse feedforward control strategy is developed to obtain a good performance for AFM Nano imaging.<sup>17</sup> A fuzzy hysteresis model, identified and optimized via uniform partition and recursive least squares, is applied to design a the feedforward controller. A hybrid control combining the controller and PID controller is favorable for canceling the hysteresis and disturbances.<sup>18</sup> A compensator, consisting of a feedforward control based on an inverse Preisach operator and feedback with a Preisach operator in the feedback path, is applied to alleviate the nonlinearity of the piezoelectric actuator.<sup>19</sup> A feedforward control based on the Prandtl-Ishlinskii model is used to compensate the hysteresis.<sup>20</sup> However, this inverse model compensation technique requires a high precision model and many hysteresis models are rate-independent. Therefore, a control strategy based on the hysteresis model is not suitable for application of frequency variation. Another compensation technique, which is independent of the hysteresis model, is a good choice to compensate for the nonlinearity of the piezoelectric actuator. Wang et al. proposed an adaptive sliding mode control based on a parameter estimation scheme to compensate for the hysteresis nonlinearity of the piezoelectric actuator.<sup>21</sup> The successful compensation of hysteresis relies on a suitable control strategy. It considers hysteresis as a disturbance or an uncertainty.<sup>22-25</sup> Liu developed an active disturbance rejection controller that treats the nonlinearity of the piezo-actuated stage as disturbance.<sup>26</sup> To further improve the tracking performances in hysteresis of PZT, several controllers are introduced. In many controllers, sliding mode control is a good choice and has been successfully employed for the piezo-actuated nano positioning stage.

Compared to the common sliding mode control, the traditional SMC with PID sliding surface can offer faster transient response and less error. The gains of the sliding function strongly affect the control performance. To further obtain a good performance, these parameters of the proposed FASMC can be adjusted online via adaptation laws. The switching control part is improved by introducing fuzzy control and adaptation law, and the signum function is replaced by a smooth function to eliminate chattering. To keep the input voltage within safety scope, an anti-saturation control is introduced into the control system. This paper is organized as follows: The fuzzy adaptive anti-saturation sliding mode controller design is presented in Section 2. Section 3 it describes the experimental set-up and the application of the proposed FASMC to the piezoelectric stage. The conclusions of the present research are summarized in Section 4.

## 2. Fuzzy Adaptive Anti-Saturation Sliding Mode Controller Design

### 2.1 Dynamic model of the piezoelectric stage

The dynamic model is the base for designing the control system. The model of the piezo-actuated nano positioning stage has been investigated in many previous studies. This structure can be equivalent to a mass-damping-spring system. The dynamic model of the moving platform and the flexure hinges is shown in Fig. 1.

In this paper, the piezo-actuated nano positioning stage consists of a mass  $m$ , a viscous damper  $c$ , and stiffness  $k$  of the moving mechanism.

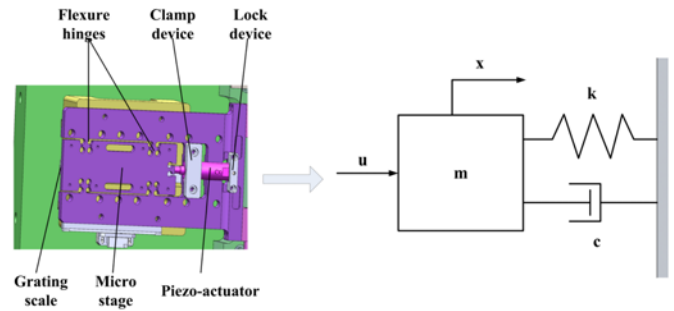


Fig. 1 Dynamic model of the piezo-actuated stage

Although the piezo-actuated system can be described by a higher-order model, a second-order model is presented due to its popularity. The dynamic equation of the piezo-actuated nano positioning stage can be obtained as

$$m\ddot{x} + c\dot{x} + kx = bu + d \quad (1)$$

where  $x$  represents the output displacement of the stage,  $u$  denotes the input voltage,  $b$  represents the coefficient, and  $d$  denotes the lumped uncertainty including hysteresis and creep. However, the lumped uncertainty has upper bound  $D$ , that is

$$d \in \Omega_d \quad \{d : |d| \leq D\} \quad (2)$$

To facilitate control design, the following form is used:

$$\ddot{x} = \frac{b}{m}u - \frac{c}{m}\dot{x} - \frac{k}{m}x + \frac{d}{m} \quad (3)$$

### 2.2 Fuzzy adaptive sliding mode control with PID sliding surface

To design the SMC, an error coordinate is defined as

$$e(t) = x_d(t) - x(t) \quad (4)$$

where  $x_d$  represents the desired state and  $e$  represents the tracking error.

The sliding surface,  $s(t)$  in the traditional SMC depends on the tracking error,  $e(t)$  and derivative of the tracking error as

$$s = \lambda e + \dot{e} \quad (5)$$

where  $\lambda$  is a positive constant.

To design a SMC with improved performance, a sliding surface of PID-type is defined as follows:

$$s = k_p e + k_i \int e(\tau) d\tau + k_d \dot{e} \quad (6)$$

In the above PID-type SMC, the slopes of the sliding function  $k_p$ ,  $k_i$ , and  $k_d$  are assigned as positive constants during the control process. Furthermore, the slopes determine the rate of decay of the tracking error. However, constant slopes may increase the oscillations in the control signal and induce the excitation of high-frequency unmodeled dynamics in the system. To overcome this weakness, variable gains with adaptive

rules are introduced into the SMC controller to change the values of the sliding function online. Therefore, the PID-type sliding function with variable gains is written as

$$s = k_p e + k_I \int_0^t e(\tau) d\tau + k_D \dot{e} \quad (7)$$

The variable gains of the PID-type sliding function are computed by the following adaption rules:

$$\begin{aligned} \dot{\hat{k}}_p &= -\eta_1 s e \\ \dot{\hat{k}}_I &= -\eta_2 s \int_0^t e(\tau) d\tau \\ \dot{\hat{k}}_D &= -\eta_3 s \dot{e} \end{aligned} \quad (8)$$

Taking the derivative of the PID-type sliding surface with respect to time and use Eq. (7), then

$$\dot{s} = \dot{\hat{k}}_p e + \hat{k}_p \dot{e} + \dot{\hat{k}}_I \int_0^t e(\tau) d\tau + \hat{k}_I e(t) + \dot{\hat{k}}_D \dot{e} + \hat{k}_D \ddot{e} \quad (9)$$

The control effort being derived as the solution of  $\dot{s} = 0$  without considering the lumped uncertainty ( $d = 0$ ) is to achieve the desired performance under the nominal model, the equivalent control  $u_{eq}$  can thus be obtained as

$$u_{eq} = \frac{m}{\hat{k}_D b} \left[ \left( \frac{\hat{k}_D c}{m} - \hat{k}_p \right) \dot{x} + \left( \frac{\hat{k}_D k}{m} - \hat{k}_I \right) x + \hat{k}_D \ddot{x}_d + \hat{k}_p \dot{x}_d + \hat{k}_I x_d \right] \quad (10)$$

In general, the switching control  $u_{sw}$  can be chosen as:<sup>27,28</sup>

$$u_{sw} = k_s \text{sign}(s) \quad (11)$$

The control law for FASMC is assumed to take the following form:

$$u = u_{eq} + u_{sw} = \frac{m}{\hat{k}_D b} \left[ \left( \frac{\hat{k}_D c}{m} - \hat{k}_p \right) \dot{x} + \left( \frac{\hat{k}_D k}{m} - \hat{k}_I \right) x + \hat{k}_D \ddot{x}_d + \hat{k}_p \dot{x}_d + \hat{k}_I x_d \right] + k_s \text{sgn}(s) \quad (12)$$

From the above description, it is concluded that the reason for the occurrence of chattering in traditional SMC lies in the existence of the  $\text{sign}$  function and the constant coefficient, and the fuzzy control is designed to replace the value of  $k_s$ . The sliding mode function  $s$  works as the input to the fuzzy control and  $\hat{k}_s$  is the output of fuzzy control. In fuzzy designing, P, Z, and N represent the fuzzy sets positive, zero and negative, respectively. Four basic fuzzy subsets are used: positive big (PB), positive medium (PM), positive small (PS) and zero (ZE). We design the following fuzzy rules:

- Rule 1: If  $s$  is P AND  $\dot{s}$  is P THEN  $\hat{k}_s$  is PB.
- Rule 2: If  $s$  is P AND  $\dot{s}$  is Z THEN  $\hat{k}_s$  is PM.
- Rule 3: If  $s$  is P AND  $\dot{s}$  is N THEN  $\hat{k}_s$  is PS.
- Rule 4: If  $s$  is Z AND  $\dot{s}$  is P THEN  $\hat{k}_s$  is PS.
- Rule 5: If  $s$  is Z AND  $\dot{s}$  is Z THEN  $\hat{k}_s$  is ZE.
- Rule 6: If  $s$  is Z AND  $\dot{s}$  is N THEN  $\hat{k}_s$  is PS.
- Rule 7: If  $s$  is N AND  $\dot{s}$  is P THEN  $\hat{k}_s$  is PS.
- Rule 8: If  $s$  is N AND  $\dot{s}$  is Z THEN  $\hat{k}_s$  is PM.
- Rule 9: If  $s$  is N AND  $\dot{s}$  is N THEN  $\hat{k}_s$  is PB.

Triangular-type functions are used to define the membership functions of the IF-part and the THEN-part. Defuzzification of the control output is realized via the method of center-of-gravity. The output fuzzy sets and the center-of-gravity defuzzification are used:

$$\Delta k_s = \frac{\sum_{i=1}^9 \theta_i \mu_i(s) \mu_i(\dot{s})}{\sum_{i=1}^9 \mu_i(s) \mu_i(\dot{s})} = \frac{\sum_{i=1}^9 \theta_i \xi_i}{\sum_{i=1}^9 \xi_i} = [\theta_1 \cdots \theta_9] \begin{bmatrix} \xi_1 \\ \vdots \\ \xi_9 \end{bmatrix} / \sum_{i=1}^9 \xi_i = \theta^T \xi(s) \quad (13)$$

where  $\mu_i$  represents the weight of the  $i$ -th rule. The equation can be rewritten as

$$\begin{aligned} \xi(s) &= [\xi_1(s), \xi_2(s), \dots, \xi_9(s)]^T \\ \xi_i(s) &= \frac{\mu_i(s) \mu_i(\dot{s})}{\sum_{i=1}^9 \mu_i(s) \mu_i(\dot{s})}, \quad \theta = [\theta_1, \theta_2, \dots, \theta_9]^T \end{aligned} \quad (14)$$

where  $\xi$  is a regressive vector and  $\theta$  is an adjustable parameter vector.

Let  $k_s^*$  be an optimal value of  $k_s$  that satisfies the existence conditions of the sliding mode, and  $k_s^*$  obtains the minimum control effort  $u_{sw}^*$ . However, in practice, the ideal controller cannot be precisely implemented. Therefore, due to  $k_s^*$ , it is very hard to obtain the precise value in advance. Consequently, employing an adaptation control system  $\hat{k}_s$  to approximate  $k_s^*$

$$\hat{k}_s = \hat{\theta}^T \xi \quad k_s^* = \theta^T \xi \quad (15)$$

For simplicity of discussion, the following form is defined:

$$\tilde{\theta} = \theta - \hat{\theta} \quad (16)$$

The adaptation law is designed as

$$\dot{\hat{\theta}} = \gamma \xi^T |s| \quad (17)$$

where  $\gamma$  represents a constant greater than 0. Since the optimal  $k_s^*$  is constant, the derivative of Eq. (15) is given as

$$\dot{\hat{k}}_s = \dot{\hat{\theta}} \quad (18)$$

This fuzzy adaptive sliding mode control can automatically calculate the control voltage.

### 2.3 Stability

Defining the Lyapunov function  $V = s^2 / 2$ , a sufficient condition for achieving stability can be given as:

$$\dot{V} = \frac{1}{2} \frac{d}{dt} s^2 = s \dot{s} \leq -\eta |s|, \quad \eta \geq 0 \quad (19)$$

where  $\eta$  represents a positive constant. The initial errors may be arbitrarily located in the error state and are generally not zero. Eq. (19) indicates that it causes the trajectories to move towards the origin. Integrating both sides over the time interval  $[0, t_s]$  and dividing by  $|s|$ , the state will be reaching the sliding surface as  $t = t_s$ , therefore

$$\int_0^{t_s} \frac{s}{|s|} \dot{s} dt \leq - \int_0^{t_s} \eta dt \quad (20)$$

$$|s(t = t_s)| - |s(t = 0)| \leq -\eta t_s \quad (21)$$

When  $|s(t_s)| = 0$ , then one has

$$t_s \leq \frac{|s(t = 0)|}{\eta} \quad (22)$$

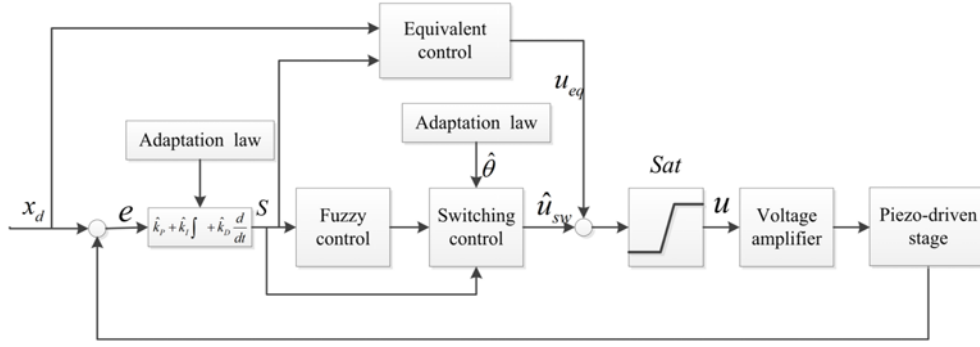


Fig. 2 Block diagram of the proposed FASMC

Therefore, the state can converge to the sliding surface within the finite time  $|s(t_s)| = 0 / \eta$ .

Consider a Lyapunov function in the following form:

$$V_2 = \frac{1}{2}ms^2 + \frac{1}{2\gamma}\hat{\theta}^2 \quad (23)$$

Substituting Eqs. (5)-(10) into (11) obtains:

$$\begin{aligned} \dot{V}_2 &= ms\dot{s} + \frac{1}{\gamma}\hat{\theta}\dot{\hat{\theta}} \\ &= -\eta_1ms^2e^2 - \eta_2ms^2\left(\int_0^t e(\tau)d\tau\right)^2 - \eta_3ms^2\dot{e}^2 \\ &\quad - k_s^*\text{sign}(s)s + ds + \frac{1}{\gamma}\hat{\theta}\dot{\hat{\theta}} \\ &= -\eta_1ms^2e^2 - \eta_2ms^2\left(\int_0^t e(\tau)d\tau\right)^2 - \eta_3ms^2\dot{e}^2 \\ &\quad - k_s^*|s| + ds + \frac{1}{\gamma}(\hat{\theta} - \hat{\theta})\gamma\xi|s| \\ &\leq -k_s^*\frac{s^2}{|s| + \varepsilon} + d|s| + \frac{1}{\gamma}(\hat{\theta} - \hat{\theta})\gamma\xi|s| \\ &\leq -k_s^*|s| + ds + \theta\xi|s| - \hat{\theta}\xi|s| \\ &\leq -(\hat{k}_s - D)|s| \\ &\leq -\eta|s| \end{aligned} \quad (24)$$

If the gain  $\hat{k}_s$  is chosen to satisfy the condition

$$\hat{k}_s \geq D + \eta \quad (25)$$

then, it can be deduced that  $\dot{V}_2$  is negative definite and satisfies Eq. (19). From the above analysis, the sliding condition is satisfied and the stability of the FASMC system is guaranteed since the derivative of the Lyapunov function is a negative definite.

The discontinuous switching function can be approximated via continuous function to avoid chattering. The new switching function with an exponentially decaying boundary layer is used to reduce chattering and improve performance. Therefore, a smoother function is introduced to substitute the signum function, thus improving the control effort as:

$$u_{sw} = k_s \frac{s}{|s| + \varepsilon} \quad (26)$$

where  $\varepsilon$  is a positive constant.

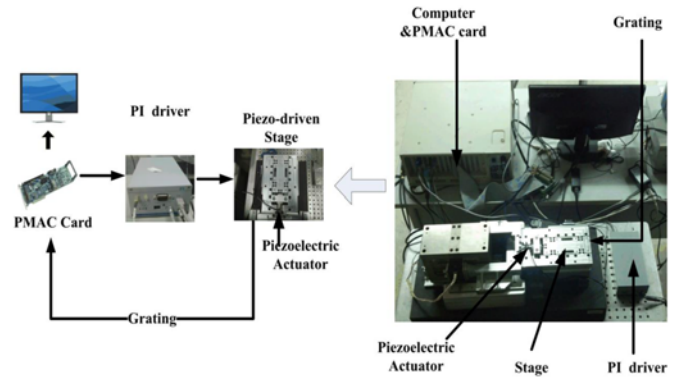


Fig. 3 Experimental platform

A block diagram of the proposed FASMC is shown in Fig. 2. Thus the control law can be written as:

$$\begin{aligned} u &= \frac{m}{\hat{k}_D b} \left[ \left( \frac{\hat{k}_D c}{m} - \hat{k}_p \right) \dot{x} + \left( \frac{\hat{k}_D k}{m} - \hat{k}_r \right) x + \right. \\ &\quad \left. \hat{k}_D \ddot{x}_d + \hat{k}_p \dot{x}_d + \hat{k}_r x_d \right] + \hat{k}_s \frac{s}{|s| + \varepsilon} \end{aligned} \quad (27)$$

In this paper, the anti-saturated control is introduced into the control input. Therefore, the control input,  $u$  is given by:

$$u = \text{sat}(u) = \begin{cases} u & |u| < u_m \\ u_m \text{sign}(u) & |u| \geq u_m \end{cases} \quad (28)$$

### 3. Experimental Results

As shown in Fig. 3, an experimental platform is built to track control of the piezo-actuated nano positioning stage. A piezoelectric actuator is adapted to drive the flexure hinges guiding positioning stage. Turbo PMAC, motion control card, generates excitation voltage signals (0-10 V) to the amplifier. The voltage signals, amplified by a high-voltage amplifier with a fixed gain of 10, are applied to the piezoelectric actuator to generate force and the stage will be actuated by the force. The output displacement is measured by grating with 10-nanometer resolution.

Creep is the expression of the slow realignment of the crystal domains in a constant voltage input over time. Fig. 4 shows the step voltage

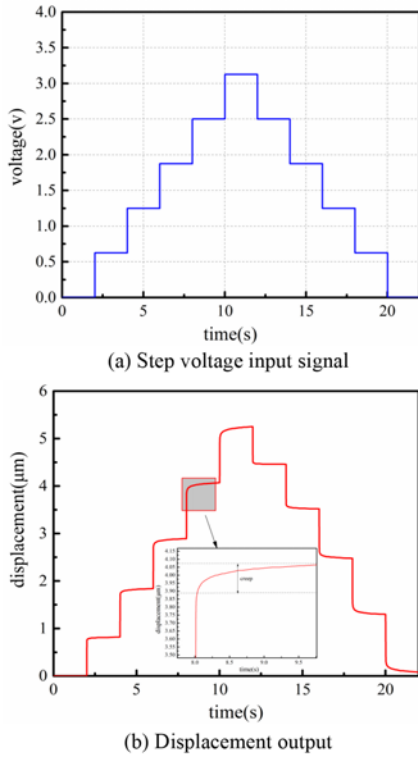


Fig. 4 Step voltage response

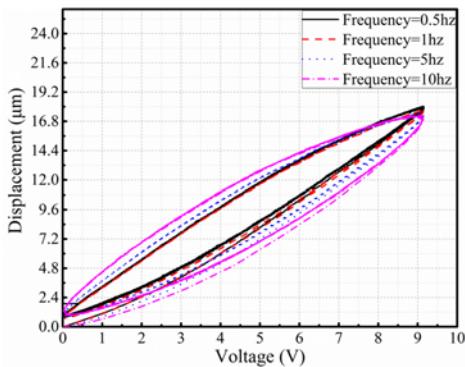


Fig. 5 Hysteresis curves of the stage with different frequencies

response of the piezo-actuated nano positioning stage. The creep phenomenon has a big impact on setting time and position precision of the piezo-actuated nano positioning stage.

The hysteresis phenomenon is a remarkable phenomenon for the piezo-actuated nano positioning stage. To demonstrate this hysteric behavior, a series of sinusoidal input voltages (0.5 Hz, 1 Hz, 5 Hz and 10 Hz) were generated via PMAC card and were applied to the piezo-actuated nano positioning stage via an open loop. The hysteresis curves obtained by the input voltage and the resulting displacement are shown in Fig. 5. Fig. 5. shows that the width of the hysteresis loop will gradually increase with increasing frequency of the input signal.

The creep and hysteresis phenomenon should be suppressed for precise positioning and improved tracking performance. Therefore, a PID controller and the proposed FASMC are applied to the piezo-actuated stage. When the input signal is a 6 μm step displacement, the parameters

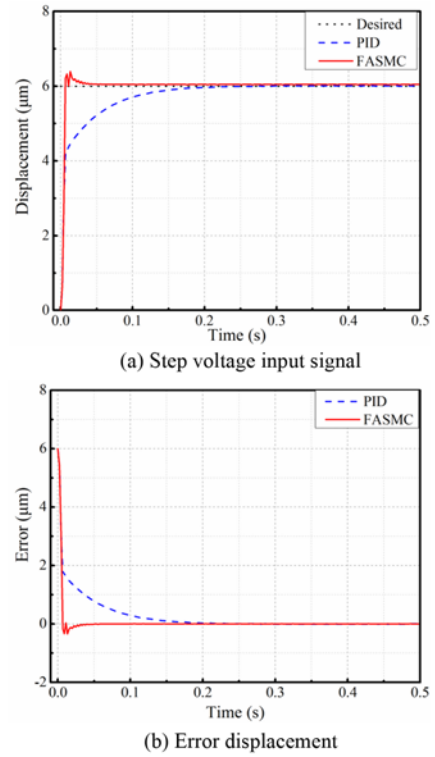


Fig. 6 Response experiment with 6 μm step input

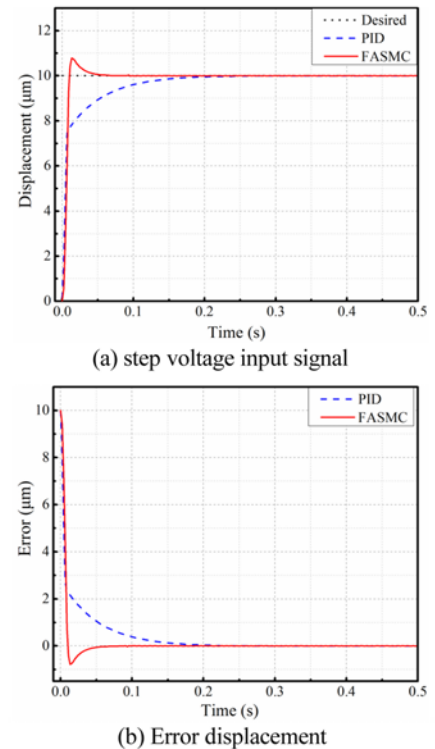


Fig. 7 Response experiment with 10 μm step input

of traditional PID controller are:  $K_{PP} = 190000$ ,  $K_{II} = 500000$ ,  $K_{DD} = 100$ . The results are shown in Fig. 6.

Experiments are performed to demonstrate improved positioning performance using the proposed FASMC. The results of 10 μm and 16

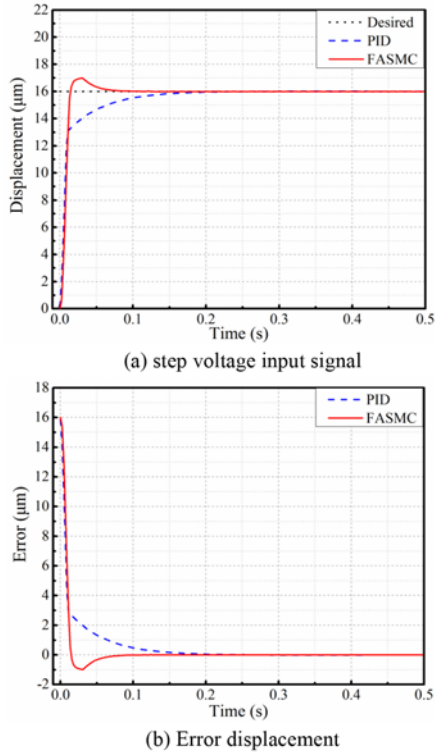


Fig. 8 Response experiment with 16  $\mu\text{m}$  step input

Table 1 Compared experimental results of step input with different controllers

Parameters		6 $\mu\text{m}$	10 $\mu\text{m}$	16 $\mu\text{m}$
Rise Time (s)	PID	0.064	0.053	0.042
	FASMC	0.005	0.009	0.012
Setting Time (s)	PID	0.144	0.136	0.119
	FASMC	0.018	0.010	0.048

Table 2 Tracking-error results of different controllers under different frequency

		Frequency			
		0.5 Hz	1 Hz	5 Hz	10 Hz
		-6 $\mu\text{m}$	-6 $\mu\text{m}$	-6 $\mu\text{m}$	-6 $\mu\text{m}$
Max Error ( $\mu\text{m}$ )	PID	0.182	0.318	1.395	2.298
	FASMC	0.057	0.049	0.164	0.317
RMS Error ( $\mu\text{m}$ )	PID	0.103	0.207	0.965	1.565
	FASMC	0.016	0.013	0.078	0.178

$\mu\text{m}$  step signals are shown in Figs. 7-8. Experimental results indicate that the proposed FASMC offers good reduction of creep and decreases both rise time and setting time. The detail compared results are described in Table 1.

In Fig. 9, the reference signal has a frequency of 0.5 Hz and an amplitude of 6  $\mu\text{m}$ . The maximum tracking error of the PID controller is 0.182  $\mu\text{m}$  and the root mean square (RMS) error is 0.103  $\mu\text{m}$ . For the proposed FASMC, the maximum tracking error is 0.057  $\mu\text{m}$  and the RMS error is 0.016  $\mu\text{m}$ . In Fig. 10, when the input reference signal has a frequency of 1 Hz and an amplitude of 6  $\mu\text{m}$ , the maximum tracking error of PID controller is 0.318  $\mu\text{m}$ ; however, the maximum error of the proposed FASMC is 0.049  $\mu\text{m}$ , while the RMS error of PID controller

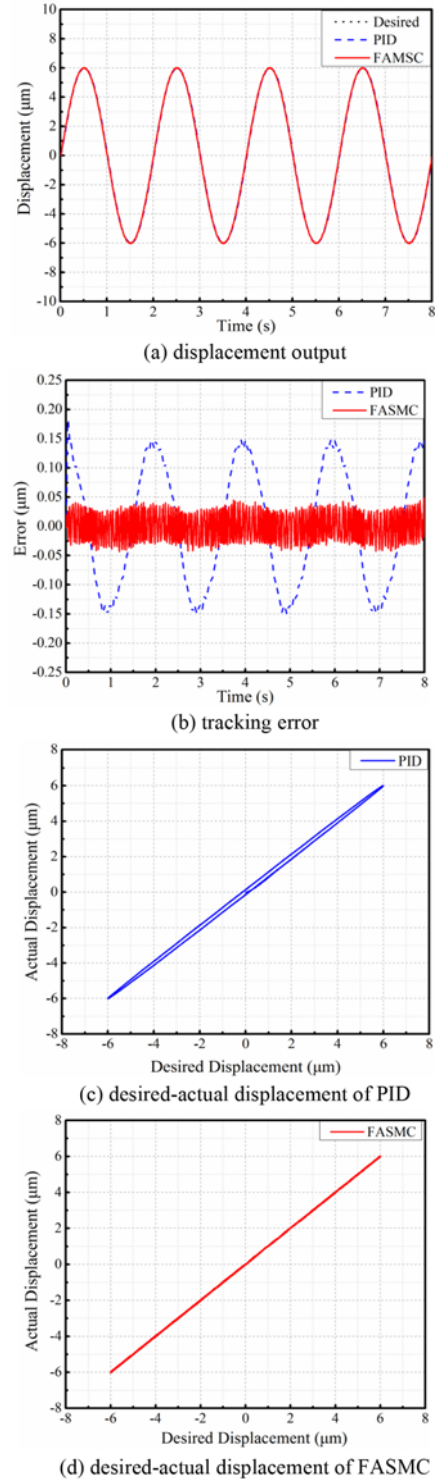


Fig. 9 Tracking results under 0.5 Hz with 6  $\mu\text{m}$  sinusoidal input

is 0.207  $\mu\text{m}$ , and the RMS error of the proposed FASMC is 0.013  $\mu\text{m}$ . The detail tracking-error results are presented in Table 2. The plots of actual displacement versus desired displacement, as shown in Figs. 9-12, indicate that the hysteresis phenomenon has been significantly compensated. Compared to Fig. 5, the width of the hysteresis loop has been reduced since the PID controller or FASMC are applied to this piezo-actuated nano positioning stage. However, Figs. 11 and 12 indicate that the hysteresis compensation of the proposed FASMC is

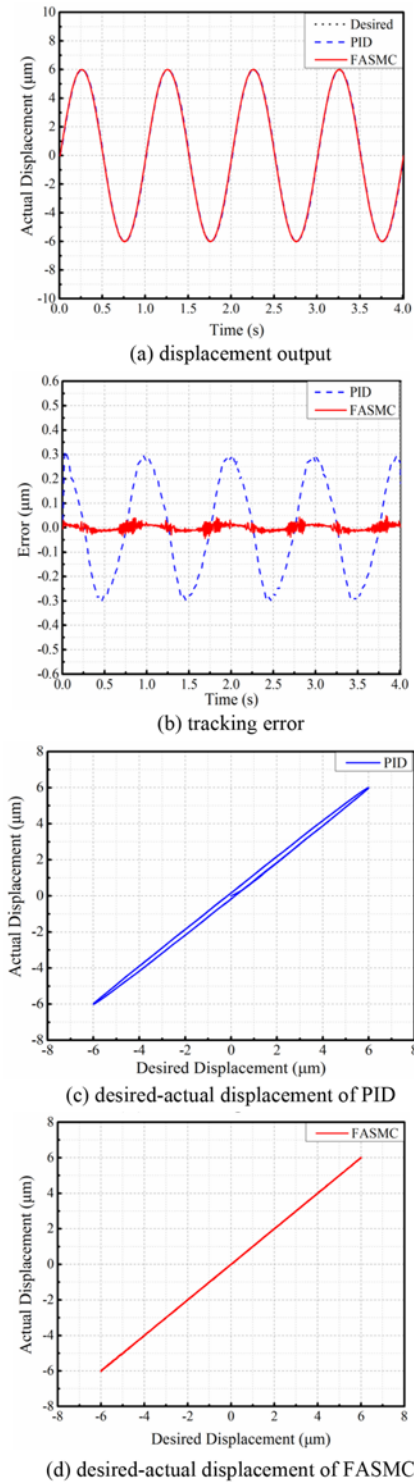


Fig. 10 Tracking results under 1 Hz with 6 μm sinusoidal input

more obvious than that of the PID controller. It can use input frequency of 10 Hz as high frequency if the piezoelectric actuator is applied for precise positioning.

When the reference signal is a signal input with a frequency of 20 Hz and 4 μm, the maximum tracking error and the RMS error of PID controller were 1.3703 μm and 0.9445 μm, respectively. However, the maximum tracking error and RMS error were 0.2465 μm and 0.1270 μm. Therefore, the FASMC can improve the tracking error (see Fig. 13).

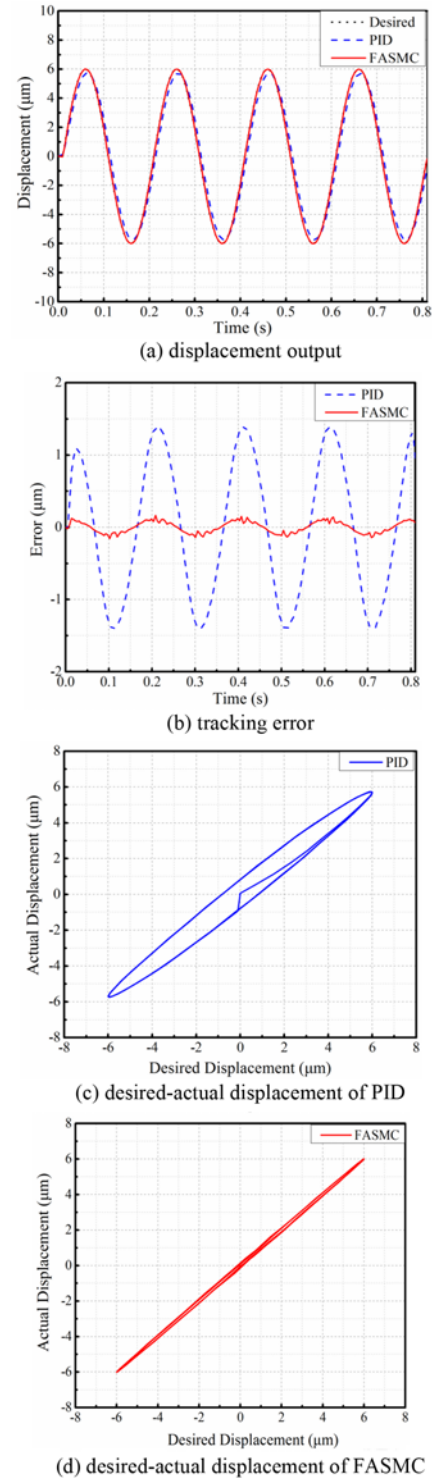


Fig. 11 Tracking results under 5 Hz with 6 μm sinusoidal input

The actual application frequency of the piezoelectric actuator is generally below 20 Hz.<sup>29</sup>

When  $y = 5 \cdot \sin(2\pi f_1 t) + 2 \cdot \sin(2\pi f_2 t)$ ,  $f_1 = 0.5$ ,  $f_2 = 5$ , a multiple frequency signal is a displacement input signal, the response is shown in Fig. 14. The maximum error is about 0.23 μm and the root-mean-square error is 0.133 μm after using FASMC; furthermore, the maximum error of using PID controller is 2.5 μm and its root-mean-square error is 1.22 μm. Therefore, the FASMC can significantly improve the

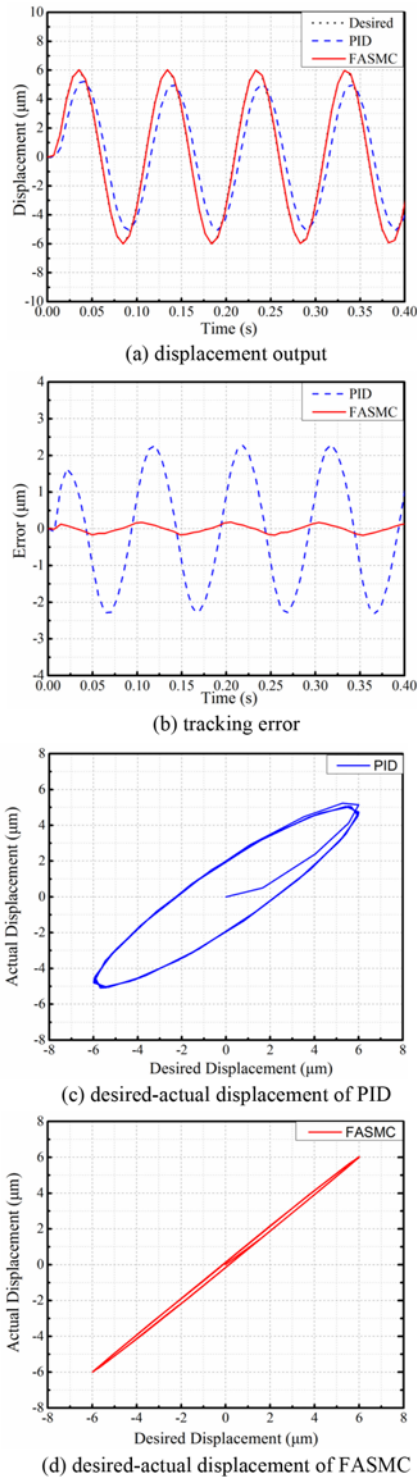


Fig. 12 Tracking results under 10 Hz with 6  $\mu\text{m}$  sinusoidal input

precision of the piezo-actuated nano positioning stage.

The tracking error of the piezo-actuated nano positioning stage will gradually increase with increasing frequency. The PID controller can also obtain good control results when the input frequency is small. With increasing frequency, its control effect will weaken. However, the proposed FASMC can always obtain favorable tracking performance. Therefore, the performance of the FASMC exceeds that of the PID controller.

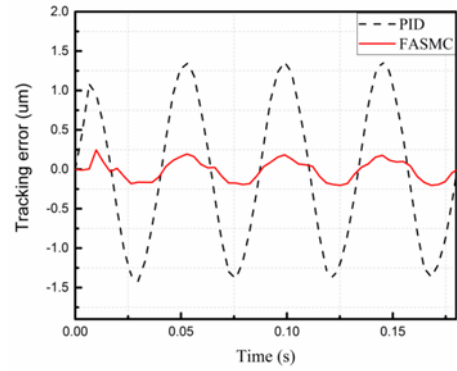


Fig. 13 Tracking results under 20 Hz with 4  $\mu\text{m}$  sinusoidal input

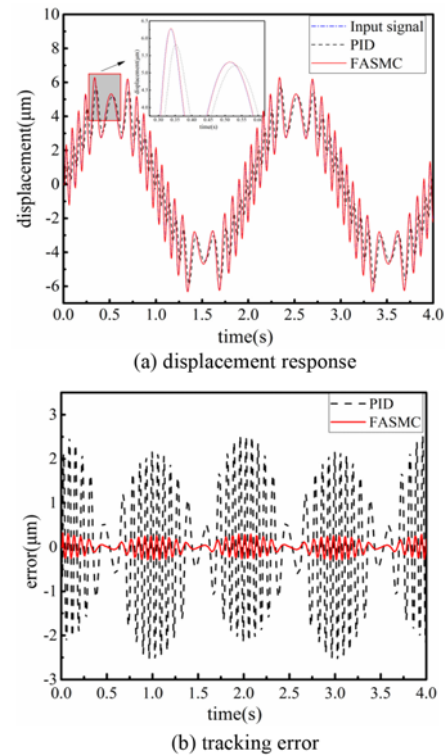


Fig. 14 Tracking results of a multiple frequency signal

#### 4. Conclusions

In this paper, an improved FASMC with PID surface is applied to the piezoelectric stage to improve tracking control. Adaptation laws are introduced to adjust the slope of the sliding function. Both fuzzy control and adaptation law are applied to tune the parameters of the switching control in the FASMC design. Due to the discontinuity of the signum function, chattering may occur in the control system. To eliminate this chattering, the switching control is modified via the smooth function. Experimental results show that both rise time and setting time are smaller with the proposed FASMC than with the PID controller. Furthermore, the proposed control can obtain improved tracking performance compared to the PID controller. The hysteresis and creep compensation effect of the FASMC is more obvious than in the PID controller.



## ACKNOWLEDGEMENT

This work was supported by the following funds: the National Natural Science Foundation of China (No.51705217, No.51705132).

The authors would like to thank Jiping Zhao, Xufei Dai and Liu-sheng for their contributions in building the experiment platform.

## REFERENCES

- Gu, G.-Y., Zhu, L.-M., Su, C.-Y., Ding, H., and Fatikow, S., "Modeling and Control of Piezo-Actuated Nanopositioning Stages: A Survey," *IEEE Transactions on Automation Science and Engineering*, Vol. 13, No. 1, pp. 313-332, 2016.
- Zhu, W., Yang, F., and Rui, X., "Robust independent Modal Space Control of a Coupled Nano-Positioning Piezo-Stage," *Mechanical Systems and Signal Processing*, Vol. 106, pp. 466-478, 2018.
- Tang, H. and Li, Y., "Design, Analysis, and Test of a Novel 2-DOF Nanopositioning System Driven by Dual Mode," *IEEE Transactions on Robotics*, Vol. 29, No. 3, pp. 650-662, 2013.
- Wang, F., Liang, C., Tian, Y., Zhao, X., and Zhang, D., "Design of a Piezoelectric-Actuated Microgripper with a Three-Stage Flexure-Based Amplification," *IEEE/ASME Transactions on Mechatronics*, Vol. 20, No. 5, pp. 2205-2213, 2015.
- Yong, Y. K., Fleming, A. J., and Moheimani, S., "A Novel Piezoelectric Strain Sensor for Simultaneous Damping and Tracking Control of a High-Speed Nanopositioner," *IEEE/ASME Transactions on Mechatronics*, Vol. 18, No. 3, pp. 1113-1121, 2013.
- Mohammadzahari, M., Grainger, S., and Bazghaleh, M., "Fuzzy Modeling of a Piezoelectric Actuator," *International Journal of Precision Engineering and Manufacturing*, Vol. 13, No. 5, pp. 663-670, 2012.
- Li, L., Li, C.-X., Gu, G., and Zhu, L.-M., "Positive Acceleration, Velocity and Position Feedback Based Damping Control Approach for Piezo-Actuated Nanopositioning Stages," *Mechatronics*, Vol. 47, pp. 97-104, 2017.
- Tang, H. and Li, Y., "A New Flexure-Based Y $\theta$  Nanomanipulator with Nanometer-Scale Resolution and Millimeter-Scale Workspace," *IEEE/ASME Transactions on Mechatronics*, Vol. 20, No. 3, pp. 1320-1330, 2015.
- Tang, H. and Li, Y., "Feedforward nonlinear PID Control of a Novel Micromanipulator Using Preisach Hysteresis Compensator," *Robotics and Computer-Integrated Manufacturing*, Vol. 34, pp. 124-132, 2015.
- Tang, H., Gao, J., Chen, X., Yu, K.-M., To, S., et al., "Development and Repetitive-Compensated PID Control of a Nanopositioning Stage with Large-Stroke and Decoupling Property," *IEEE Transactions on Industrial Electronics*, Vol. 65, No. 5, pp. 3995-4005, 2018.
- Hassani, V., Tjahjowidodo, T., and Do, T. N., "A Survey on Hysteresis Modeling, Identification and Control," *Mechanical Systems and Signal Processing*, Vol. 49, Nos. 1-2, pp. 209-233, 2014.
- Nguyen, P.-B. and Choi, S.-B., "Open-Loop Position Tracking Control of a Piezoceramic Flexible Beam Using a Dynamic Hysteresis Compensator," *Smart Materials and Structures*, Vol. 19, No. 12, Paper No. 125008, 2010.
- Gu, G.-Y. and Zhu, L.-M., "Comparative Experiments Regarding Approaches to Feedforward Hysteresis Compensation for Piezoceramic Actuators," *Smart Materials and Structures*, Vol. 23, No. 9, Paper No. 095029, 2014.
- Liu, Y., Shan, J., Gabbert, U., and Qi, N., "Hysteresis and Creep Modeling and Compensation for a Piezoelectric Actuator Using a Fractional-Order Maxwell Resistive Capacitor Approach," *Smart Materials and Structures*, Vol. 22, No. 11, Paper No. 115020, 2013.
- Zhu, W. and Rui, X.-T., "Hysteresis Modeling and Displacement Control of Piezoelectric Actuators with the Frequency-Dependent Behavior Using a Generalized Bouc-Wen Model," *Precision Engineering*, Vol. 43, pp. 299-307, 2016.
- Eielsen, A. A., Gravdahl, J. T., and Pettersen, K. Y., "Adaptive Feed-Forward Hysteresis Compensation for Piezoelectric Actuators," *Review of Scientific Instruments*, Vol. 83, No. 8, Paper No. 085001, 2012.
- Tang, H., Li, Y., and Zhao, X., "Hysteresis Modeling and Inverse Feedforward Control of an AFM Piezoelectric Scanner Based on Nano Images," *Proc. of International Conference on Mechatronics and Automation (ICMA)*, pp. 189-194, 2011.
- Li, P., Yan, F., Ge, C., and Zhang, M., "Ultra-Precise Tracking Control of Piezoelectric Actuators Via a Fuzzy Hysteresis Model," *Review of Scientific Instruments*, Vol. 83, No. 8, Paper No. 085114, 2012.
- Kuhnen, K. and Krejci, P., "Compensation of Complex Hysteresis and Creep Effects in Piezoelectrically Actuated Systems — A New Preisach Modeling Approach," *IEEE Transactions on Automatic Control*, Vol. 54, No. 3, pp. 537-550, 2009.
- Shan, Y. and Leang, K. K., "Accounting for Hysteresis in Repetitive Control Design: Nanopositioning Example," *Automatica*, Vol. 48, No. 8, pp. 1751-1758, 2012.
- Wang, G. and Xu, Q., "Design and Precision Position/Force Control of a Piezo-Driven Microinjection System," *IEEE/ASME Transactions on Mechatronics*, Vol. 22, No. 4, pp. 1744-1754, 2017.
- Cao, Y. and Chen, X., "A Survey of Modeling and Control Issues for Piezo-Electric Actuators," *Journal of Dynamic Systems, Measurement, and Control*, Vol. 137, No. 1, Paper No. 014001, 2015.
- Peng, J. Y. and Chen, X. B., "Integrated PID-Based Sliding Mode State Estimation and Control for Piezoelectric Actuators," *IEEE/ASME Transactions on Mechatronics*, Vol. 19, No. 1, pp. 88-99, 2014.
- Yi, J., Chang, S., and Shen, Y., "Disturbance-Observer-Based Hysteresis Compensation for Piezoelectric Actuators," *IEEE/ASME Transactions on Mechatronics*, Vol. 14, No. 4, pp. 456-464, 2009.

25. Xu, Q., "Identification and Compensation of Piezoelectric Hysteresis without Modeling Hysteresis Inverse," *IEEE Transactions on Industrial Electronics*, Vol. 60, No. 9, pp. 3927-3937, 2013.
26. Liu, P.-B., Yan, P., Zhang, Z., and Leng, T.-T., "Flexure-Hinges Guided Nano-Stage for Precision Manipulations: Design, Modeling and Control," *International Journal of Precision Engineering and Manufacturing*, Vol. 16, No. 11, pp. 2245-2254, 2015.
27. Eker, İ., "Second-Order Sliding Mode Control with Experimental Application," *ISA Transactions*, Vol. 49, No. 3, pp. 394-405, 2010.
28. Shen, J.-C., Lu, Q.-Z., Wu, C.-H., and Jywe, W.-Y., "Sliding-Mode Tracking Control with DNLRX Model-Based Friction Compensation for the Precision Stage," *IEEE/ASME Transactions on Mechatronics*, Vol. 19, No. 2, pp. 788-797, 2014.
29. Wang, X., "Research Based on Piezoelectric Ceramics Hysteresis Nonlinear Modeling and Control," Ph.D. Thesis, Harbin Engineering University, 2010.



#### **Michael Yu Wang**

Michael Yu Wang - received the Ph.D. degree in mechanical engineering from Carnegie Mellon University, Pittsburgh, PA, in 1989. Prof. Wang is currently working in the HongKong University of Science and Technology. He is a Fellow of ASME, HKIE and IEEE. His research interests include precision fixturing and grasping, particle vibration damping for electronics manufacturing, computational design and modeling, and development of 3D microstructures.  
E-mail: mywang@ust.hk



#### **Jiwen Fang**

Jiwen Fang – received the Ph.D. degree in Xi'an Jiaotong University. He joined School of Mechanism Engineering, Jiangsu University of Science and Technology, China, in 2016. His research interest is motion control, the hysteresis compensating control of piezo-actuator and soft robot.  
E-mail: fjw617@just.edu.cn



#### **Lufan Zhang**

Lufan Zhang – received the Ph.D. degree in Xi'an Jiaotong University. He joined the School of Mechanic and Electrical Engineering, Henan University of Technology, Zhengzhou, China, in 2015. His research interest is mechanically design and optimization.  
E-mail: zzzhanglufan @163.com



#### **Zhili Long**

Zhili Long - received a B.S. degree and Ph.D. degree in mechanical engineering from Central South University, Hunan, China in 2003 and 2007, He has been working as associate professor in Harbin Institute of Technology Shenzhen Graduate School. His research interests include are machinery and equipment dynamics and vibration control, piezoelectric devices with ultrasonic system design and control, precision machine design and so on.  
E-mail: longworking@163.com